

# Imine bonding self-repair hydrogels after periodate-triggered breakage of their cross-links

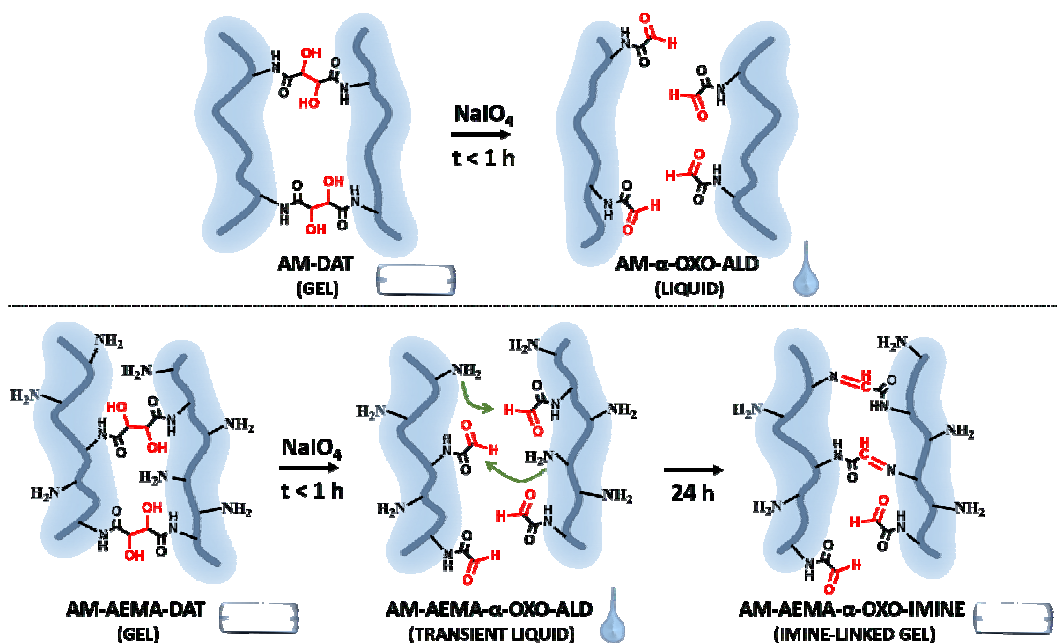
Alexis Wolfel, Cecilia Inés Alvarez Igarzabal, and Marcelo R. Romero\*

Laboratorio de Materiales Poliméricos (LAMAP), Departamento de Química Orgánica,  
Universidad Nacional de Córdoba, Instituto Investigación en Ingeniería de Procesos y Química  
Aplicada (IPQA-CONICET), Haya de la Torre y Medina Allende, Córdoba, Argentina.

\*marceloricardoromero@gmail.com

Phone: (54) 0351-5353867/69

## GRAPHICAL ABSTRACT



## ABSTRACT

1 The development of new materials with smart properties is currently expanding the  
2 development of new technologies. Therefore, the design of materials with novel  
3 sensitivities and smart behavior is important for the development of smart systems with  
4 automated responsivity. We have recently reported the synthesis of hydrogels, cross-  
5 linked by *N,N'*-diallyltartardiamide (DAT). The covalent DAT-crosslinking points have  
6 vicinal diols which can be easily cleaved with periodate, generating changes in the  
7 hydrogel properties, as well as generating valuable  $\alpha$ -oxo-aldehyde functional groups  
8 useful for further chemical modification. Based on those findings, we envisioned that a  
9 self-healable hydrogel could be obtained by incorporation of primary amino functional  
10 groups, from 2-aminoethyl methacrylate hydrochloride (AEMA), coexisting with DAT into  
11 the same network. Herein,  $\alpha$ -oxo-aldehyde groups generated after the reaction with  
12 periodate would arise in the immediate environment of amine groups to form imine  
13 cross-links. For this purpose, DAT-crosslinked hydrogels were synthesized and carefully  
14 characterized. The cleavage of DAT-crosslinks with periodate promoted changes in the  
15 mechanical and swelling properties of the materials. As expected, a self-healing  
16 behavior was observed, based on the spontaneous formation of imine covalent bonds.  
17 In addition, we surprisingly found a combination of fast vicinal diols cleavage and a low  
18 speed self-crosslinking reaction by imine formation. Consequently, it was found a time-  
19 window in which a periodate-treated polymer was obtained in a transient liquid state,  
20 which can be exploited to choose the final shape of the material, before automated  
21 gelling. The singular properties attained on these hydrogels could be useful for  
22 developing sensors, actuators, among other smart systems.

1 **Keywords: self-healing, imine, Schiff base, periodate, diol, *N,N'*-diallyltartardiamide,**  
2  **$\alpha$ -oxoaldehyde,2-aminoethyl methacrylate**

3

#### 4 **1. INTRODUCTION**

5 Smart hydrogels (HG) can change their properties in a functional and predictable  
6 manner in response to external stimuli.<sup>1</sup> This stimuli-responsive behavior expanded  
7 their potential applications by the amplification of their sensitivity to a wide range of  
8 stimulus, and promoting different smart-responsiveness such as: sol-gel transitions,  
9 volume phase transitions; changes on the mechanical or swelling properties, or in the  
10 color, modifications on their conductivity, among others.<sup>2</sup> During the last decade, a new  
11 generation of smart-materials gained much attention showing advanced properties such  
12 as self-healing and shape memory.<sup>2,3</sup> In HGs, these properties are usually achieved by  
13 a combination of stable and dynamic bonds (secondary, covalent, or supramolecular),  
14 which can generate new linkages upon an external damage and/or triggered by an  
15 external stimulus, to repair the material, and/or to recover a predefined shape.<sup>4</sup>  
16 Moreover, for some self-healing materials, the curing ability can be selectively triggered  
17 by environmental stimulus (non-autonomic self-healing) such as changes in: moisture  
18 content<sup>5</sup>; pH<sup>6</sup>; UV-light<sup>7</sup>; among others<sup>8</sup>; which can be useful for particular applications  
19 such as tissue engineering<sup>9</sup> or 3D-printing<sup>8</sup>.

20 In particular, the adaptability of strong interactions such as covalent bonds, modifying  
21 the molecular architecture of materials in response to external stimuli, is one of the  
22 current challenges.<sup>10,11</sup> These bonds can improve the ability of materials to withstand  
23 mechanical stress and also provide intelligent properties for uses as sensors/actuators,  
24 *in-situ* gelling materials, tissue engineering, controlled-release of bioactive drugs,

1 among others.<sup>4,10,12,13</sup> In this respect, imine bonds ( $\text{RN}=\text{CR}_2$ ; with R = H and / or  
2 hydrocarbyl) are formed by reaction of an amino functional group (FG) with a ketone or  
3 an aldehyde, and usually show a reversible behavior in aqueous solution.<sup>14</sup> The  
4 reversible imine bond formation/hydrolysis is highly dependent on the environmental  
5 conditions and the chemical nature of the participant molecules.<sup>15</sup> Furthermore, imine  
6 formation is usually achieved with high selectivity and specificity at physiological  
7 conditions, and is then widely used for bioconjugation.<sup>16,17</sup> Moreover, these bonds have  
8 been exploited for the development of HGs with self-healing<sup>18,19</sup> and shape memory<sup>20</sup>  
9 properties; injectable type<sup>21</sup>, with the possibility of releasing drugs in a controlled  
10 manner<sup>22</sup>; among others. However, the incorporation of imine cross-links into HGs  
11 based on vinylic monomers usually involves the difficulty of obtaining the reactive  
12 precursors into the network. Whereas amine FGs can be easily obtained by  
13 incorporating amino vinylic monomers, on the contrary, the aldehyde functionalization  
14 represents a challenge. Aldehyde bearing monomers are usually toxic and unstable  
15 under polymerization conditions, making necessary to protect the aldehyde FG.<sup>23</sup>  
16 Typically, this procedure involves several reaction steps to introduce and remove the  
17 protecting groups. As a straightforward protocol, we have previously demonstrated the  
18 use of an effortless post-synthesis modification of the cross-linker  
19 *N,N'*-diallyltartardiamide (DAT) to obtain valuable  $\alpha$ -oxoaldehyde FGs.<sup>24</sup> This  
20 modification is promoted by the periodate-mediated cleavage of diol FGs, a quick  
21 reaction that is mild enough to be used on living cells.<sup>25-27</sup> The combination of those  
22  $\alpha$ -oxoaldehyde groups with amino FGs into hydrogel networks, could open a window for  
23 an easy yield of chemoselective imine covalent linkages in HGs. The reactivity of  $\alpha$ -oxo-

1 aldehyde with amine groups in synthetic polymers, only has scarce antecedents in  
2 which DAT cross-linker was used for immobilization of ligands in polymeric matrices by  
3 reductive amination.<sup>28–30</sup> The coexistence of  $\alpha$ -oxo-aldehyde with amino FGs in  
4 polymeric networks, to generate imine as cross-linking points, could give rise to  
5 materials with properties such as shape memory, sol-gel transitions and self-healing.  
6 Furthermore, the chemoselectivity of imine bond formation could enable the gelation  
7 under physiological conditions and the immobilization of biomolecules and/or drugs for  
8 biomedical applications.<sup>31</sup>

9 As previously mentioned, amino FGs can be included by free radical polymerization of  
10 vinyl monomers such as 2-aminoethyl methacrylate monomer (AEMA). The  
11 homopolymer poly-(2-aminoethyl methacrylate) (p-AEMA) and its copolymer with *N,N'*-  
12 methylenebis(acrylamide) (BIS) have proven biocompatibility.<sup>32,33</sup> In addition, the amino  
13 FG introduced by AEMA have been used to include useful modifications on different  
14 materials. In some cases, it was used for conjugation with aldehyde or ketone FGs  
15 through the formation of imines. For example, for the immobilization of functional  
16 molecules into synthetic polymers, for applications such as antifungal materials<sup>34</sup>; waste  
17 water treatment<sup>35</sup>; or development of polymeric inks<sup>36</sup>.

18 In line with the above considerations, herein we propose the obtainment of self-healing  
19 HGs based on acrylamide (AM) and AEMA, covalently cross-linked with DAT, alone or  
20 together with BIS. After the characterization of the effects caused by the incorporation of  
21 DAT and AEMA, the HGs were treated with an aqueous solution of sodium periodate, at  
22 room temperature, to broke DAT-crosslinks and yield aldehyde pendant groups. Then, a  
23 self-healing process was observed in the hydrogels, caused by the formation of new

1 imine bonds. The automatic reparation of the network demonstrated the potential of this  
2 chemical strategy for the yield of covalently bonded self-healing materials which could  
3 be useful in several applications.

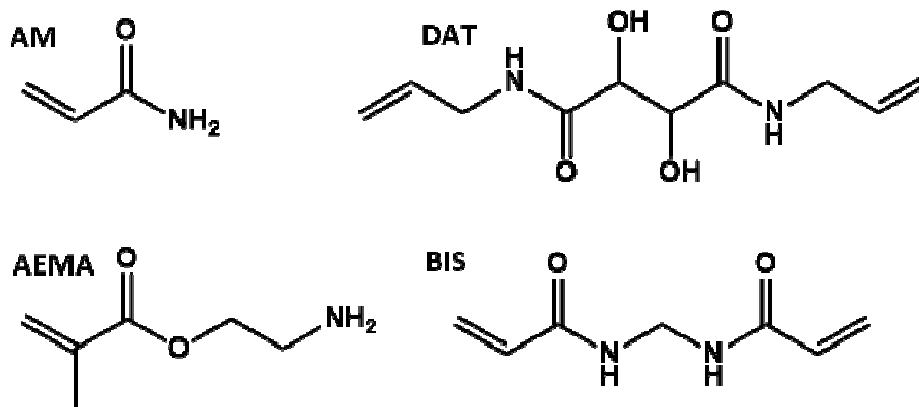
4

## 5 **2. MATERIALS AND METHODS**

### 6 **2.1 Reagents**

7 For the synthesis of HGs, acrylamide (AM), 2-aminoethylmethacrylate hydrochloride  
8 (AEMA), and both cross-linking agents, (+)-*N,N'*-diallyltartardiamide (DAT) and *N,N'*-  
9 methylenebisacrylamide (BIS) (Figure 1) (*Aldrich*), were used. The polymerization  
10 reaction was initiated with ammonium persulfate (APS) (*Anedra*), and the activator  
11 *N,N,N',N'*-tetramethylethylenediamine (TEMED) (*Aldrich*). The HGs were modified with  
12 sodium periodate (NaIO<sub>4</sub>) (*Aldrich*). Picryl sulfonic acid (TNBS) (*Sigma*), in a  
13 concentration of 5% (w/v) in H<sub>2</sub>O, was used for the identification test of amine groups.  
14 All the reagents were used as received. The solutions were prepared with ultra-pure  
15 water (18MΩcm<sup>-1</sup>).

16



17

18

Figure 1. Reagents used in the synthesis of hydrogels (HG).

19

## 2.2 SYNTHESIS

The HGs were prepared by free radical polymerization. For this, the monomers AM:AEMA in a molar ratio of 95:5 (7 mmol in total), different quantities of cross-linking agents (see Table 1) and APS (0.26 mmol) were dissolved in ultrapure water to a final volume of 5 mL, in a vial with a rubber cap. Then, each solution was cooled in an ice water bath and deoxygenated by bubbling N<sub>2</sub> for 10 min. To start the polymerization, 0.5 mL of a TEMED solution (0.32 M) was added to the vial, and each solution was transferred to 5 mL disposable syringes. The syringes were placed in a thermal water bath at 50 °C for 16 h. Finally, the HGs were cut into discs of 3 mm thick and 12 mm in diameter and washed thoroughly with water.

Table 1. Composition of the synthesized HGs.

<i>Nomenclature</i>	<i>AM:AEMA mol ratio</i>	<i>Cross-linkers (%)*</i>
<i>p-AM-AEMA-BIS</i>	95:5	BIS (5) - DAT (0)
<i>p-AM-AEMA-BIS-DAT(1)</i>	95:5	BIS (5) - DAT (1)
<i>p-AM-AEMA-BIS-DAT(3)</i>	95:5	BIS (5) - DAT (3)
<i>p-AM-AEMA-BIS-DAT(5)</i>	95:5	BIS (5) - DAT (5)
<i>p-AM-AEMA-BIS-DAT(7)</i>	95:5	BIS (5) - DAT (7)
<i>p-AM-AEMA-BIS-DAT(10)</i>	95:5	BIS (5) - DAT (10)
<i>p-AM-BIS-DAT(10)</i>	100:0	BIS (5) - DAT (10)
<i>p-AM-AEMA-DAT(10)</i>	95:5	BIS (0) - DAT (10)
<i>p-AM-DAT(10)</i>	100:0	BIS (0) - DAT (10)

\*Molar percentage with respect to total moles of monomers.

1

## 2 **2.3 POST-SYNTHETIC MODIFICATION OF HGs**

### 3 **2.3.1 Treatment of p-AM-AEMA-BIS-DAT with periodate**

4 The HG discs were dried in an oven at 37 °C ( $\approx$  80 mg of dried mass). Then, they were  
5 swelled in 50 mL of water for 3 days. Once attained equilibrium, they were placed in  
6 vials containing 1.5 mL of 0.2 M sodium periodate solution and stirred in an orbital  
7 oscillator for 1 h. The reaction was quenched by adding 2 mL of 4 % v/v glycerol  
8 solution. Then, the discs were thoroughly washed with distilled water. For swelling rate  
9 measurements (SR, see Section 2.4.1) during the reaction, a similar procedure was  
10 followed, without the addition of glycerol; the mass was measured every hour  
11 gravimetrically.

12

### 13 **2.3.2 Total degradation of cross-links and gel self-healing**

14 HGs synthesized using only DAT as a cross-linker (p-AM-DAT and p-AM-AEMA-DAT,  
15 see Table 1) were submitted to total degradation of their cross-links. Previously, the  
16 dried gel discs ( $\approx$  80 mg of dried mass) were swelled to equilibrium in water, and placed  
17 in vials. To perform the total degradation, 1.25 mL of 0.1 M NaIO<sub>4</sub> solution was added,  
18 estimating excess of the oxidant. Then, the self-curing behavior of the fully degraded  
19 products was analyzed. The total degradation phenomenon was filmed and processed  
20 with the mobile application “Framelapse” [Singh, N. (2017), Framelapse - Time Lapse  
21 Camera(4.1)-  
22 Mobileapplicationsoftware.Retrievedfrom[https://play.google.com/store/apps/details?id=c  
23 om.Nishant.Singh.DroidTimelapse](https://play.google.com/store/apps/details?id=com.Nishant.Singh.DroidTimelapse)]. esto no tiene espacio, no se puede separar?

24



### 1 **2.3.3 Amine detection by a coloration test with TNBS**

2 For the identification of amino groups, pieces of the different HGs (about 50 mg of  
3 swollen mass) fully swollen in water, were immersed into 1 mL of saturated solution of  
4 sodium borate for 1 h. Subsequently, 90  $\mu\text{L}$  of 1.5 % w/v TNBS solution in ethanol was  
5 added. After 3 h, photographs of the tested materials were recorded.

6

## 7 **2.4 CHARACTERIZATION OF THE HGs**

### 8 **2.4.1 Swelling studies**

9 The HGs discs ( $\approx$  80 mg of dried mass) were swollen in distilled water (250 mL) in a  
10 beaker, at 20  $^{\circ}\text{C}$  for three days, until reaching constant mass. The mass of the  
11 dehydrated products was obtained by drying the discs in an oven at 37  $^{\circ}\text{C}$  until constant  
12 weight.

13 The equilibrium swelling ratio (ESR) was calculated according to Equation 1.<sup>37</sup>

14

$$15 \text{ ESR} = (m_e - m_s) / m_s \quad \text{(Equation 1)}$$

16

17 Where  $m_e$  is the mass of the gel in its swelling equilibrium, and  $m_s$  corresponds to the  
18 mass of dry hydrogel.

19 The swelling kinetic of the HGs was studied by determining the swelling rate (SR) at  
20 different times. To perform this study, the dehydrated discs ( $\approx$  80 mg of dried mass)  
21 were submerged in water (250 mL) in a beaker, and the weight changes were recorded  
22 as a function of time, until a constant mass was reached. The SR was calculated using  
23 Equation 2, where  $m_t$  corresponds to the gel mass at a certain time [14]:

24

1  $SR = (m_t - m_s) / m_s$  (Equation 2)

2

3 Based on the swelling kinetic of the HGs, the type of water diffusion within the matrix  
4 was estimated using the Equation 3:

5

6  $M_t / M_\infty = vt^n$  (Equation 3)

7

8 Where  $M_t$  corresponds to the mass of water incorporated into the sample at time  $t$ ;  $M_\infty$  is  
9 the mass of water incorporated into the gel at equilibrium, and  $v$  is a constant related to  
10 the structure of the network. The exponent  $n$  is a number related to the type of diffusion.  
11 This equation is applicable only during the onset of swelling, when it is less than 60% of  
12 equilibrium. The value of  $n$  and  $v$  were obtained from the slope and intercept of the  
13 curve  $\ln (M_t / M_\infty)$  vs.  $\ln t$ .<sup>37</sup>

14

#### 15 **2.4.2 Infrared spectroscopy (FT-IR) and nuclear magnetic resonance (NMR)**

16 The samples were analyzed by infrared spectroscopy (FT-IR) in a Nicolet 5-SXC FTIR  
17 Spectrometer. Discs were prepared by mixing about 2 mg of xerogel or dehydrated  
18 monomer and 100 mg of KBr. The mixture was pulverized in a mortar and then  
19 compacted into a thin disk using a 10 Ton hydraulic press. The FT-IR spectra were  
20 acquired in the spectral range of 4000-400  $\text{cm}^{-1}$  with a resolution of 4  $\text{cm}^{-1}$  using 64  
21 scans per sample.

22 The  $^1\text{H}$ -NMR and  $^{13}\text{C}$ -NMR spectra were obtained on a 400 MHz Bruker Advance  
23 Nuclear Magnetic Resonance Spectrometer (USA) using dried and ground samples,  
24 subsequently swollen in  $\text{D}_2\text{O}$ .

1  
2  
3  
4  
5  
6  
7  
8  
9  
10  
11  
12  
13  
14  
15  
16  
17  
18  
19  
20  
21  
22  
23  
24

### 3. RESULTS AND DISCUSSION

Copolymers of acrylamide (AM) and 2-aminoethyl methacrylate (AEMA) cross-linked in absence or presence of BIS (5 mol%, respect to total moles of monomers) and different DAT amounts (0; 1; 3; 5; 7 and 10 mol%) were synthesized, as indicated in Table 1. In all cases, HGs with good mechanical properties, easy to handle without generating visible damages, were obtained.

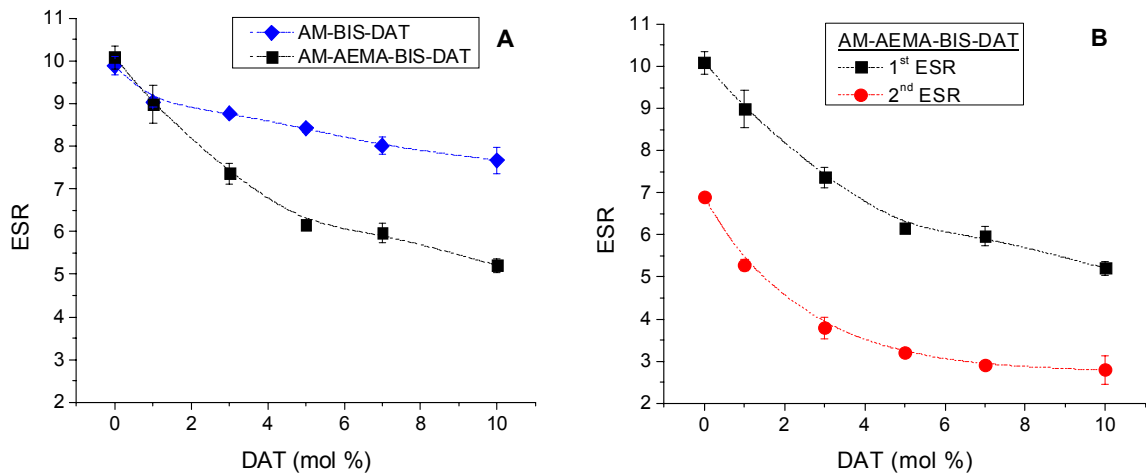
We have previously reported the synthesis of AM-BIS-DAT HGs where the periodate mediated cleavage of DAT-crosslinks caused the formation of aldehyde FGs in the network.<sup>24</sup>In this work, we aimed to enhance their smart properties by incorporating an imine based self-healing behavior which could be triggered by periodate. Thus, AEMA incorporation was needed for obtaining amines in the network that would later be combined with the aldehyde FGs that could be formed by the presence of periodate. However, AEMA incorporation could modify the delicate balance which controls the swelling equilibrium of HGs,by affecting the hydrophilicity of the polymers, the interactions between polymer chains (covalent or non-covalent) or even the reactivity of the system during polymerization conditions. Therefore, swelling studies were performed to verify the effect of using different amounts of cross-linker DAT in the equilibrium swelling rate (ESR) of the HGs containing AEMA (AM-AEMA-BIS-DAT), and were compared with those in absence of AEMA (AM-BIS-DAT) (Figure 2). In general, the marked decrease in ESR with the increase in %DAT (Figure 2A) evidenced an efficient incorporation of a greater number of covalent cross-links in both systems. These cross-links act as "knots" between network chains, limiting the capacity of expansion of the gel and restricting the absorption of higher volumes of solvent.

1 However, AEMA containing networks showed a reduction of ESR when the  
2 concentration of DAT increased, indicating strong secondary interactions between  
3 AEMA and DAT in the network, or an effect on the reactivity of the crosslinker in  
4 presence of AEMA.

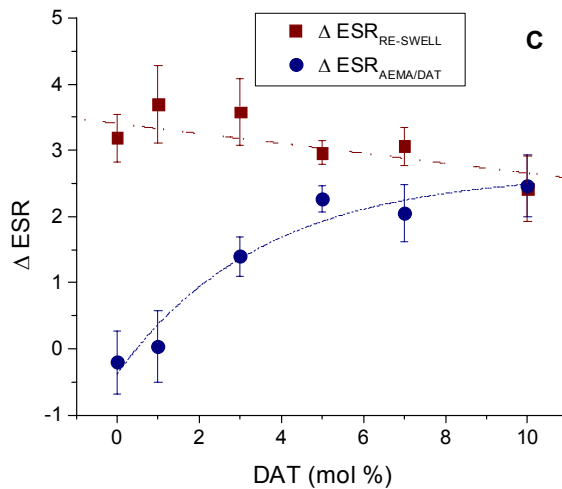
5 To study the effect of physical interactions between polymer chains, AM-AEMA-BIS-  
6 DAT HGs were dried at 37 °C until constant weight, and then swelled again in water for  
7 3 days. Figure 2B shows the values indicated as 1<sup>st</sup> ESR, corresponding to swelling of  
8 the gels equilibrated in water after the synthesis (in which the polymer chains have  
9 never been dehydrated), and 2<sup>nd</sup> ESR, corresponding to dried and re-swollen HGs.  
10 During drying, the absence of solvent allows the chains to interact intimately with each  
11 other. This approach typically promotes the formation of amorphous and/or crystalline  
12 domains, hard to solvate with water. For this reason, the 2<sup>nd</sup> ESR decreases respect to  
13 the 1<sup>st</sup> ESR for all the samples. In effect, new domains act as pseudo-crosslinks, limiting  
14 the access of solvent, and therefore their swelling capacity. It is noteworthy that the  
15 decrease in ESR produced by non-covalent interactions is practically independent of  
16 DAT concentration. Therefore, the change in ESR upon drying and re-swelling  
17 ( $\Delta ESR_{RE-SWELL} = 1^{st} ESR_{AM-AEMA-BIS-DAT} - 2^{nd} ESR_{AM-AEMA-BIS-DAT}$ ) only shows a small  
18 decreasing curve (black squares in Figure 2C), which could be related to a lesser  
19 capability to form stable non-covalent domains, due to the reduced chain mobility,  
20 promoted by the higher cross-linking degree. The almost DAT-independent ESR  
21 diminution observed, indicates that AEMA and DAT do not form particularly strong  
22 interactions, which may be expected to be increased in number during the drying and  
23 re-swelling process. Therefore, the marked DAT-dependent ESR diminution of AEMA

1 containing HGs, with respect to HGs in absence of AEMA ( $\Delta ESR_{AEMA/DAT} = ESR_{AM-BIS-DAT} - ESR_{AM-AEMA-BIS-DAT}$ , red circles in Figure 2C) could be better related to an increase  
 2 in the incorporation of DAT as crosslinker (i.e. by reaction of both vinyl ends), when  
 3 AEMA is present.  
 4

5



6



7

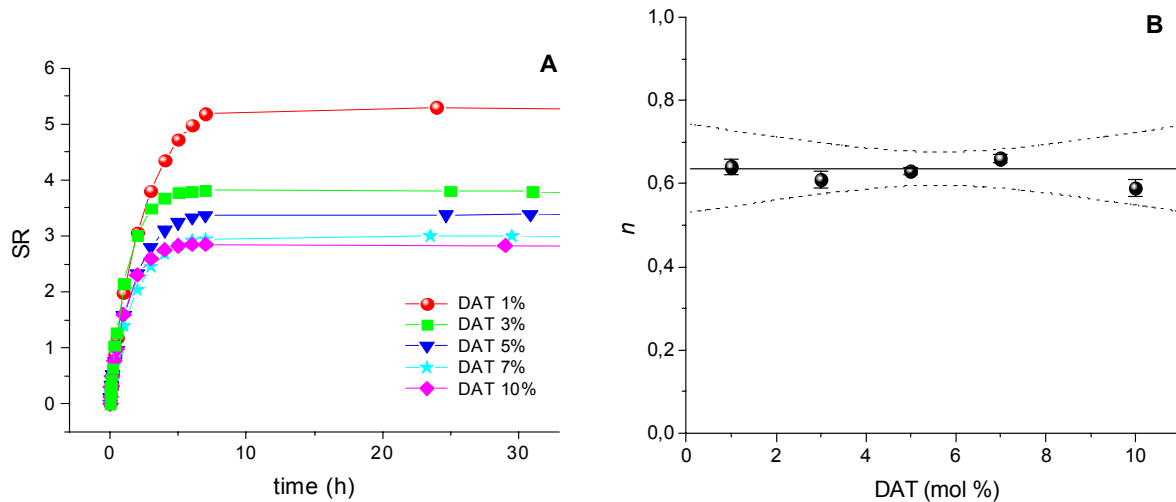
8 **Figure 2.A) Comparison of ESR of HGs, synthesized with (black squares) or without (blue**  
 9 **rhombus) AEMA, with respect to %DAT (mol%); B) Dependence on swelling capacity with %DAT**  
 10 **after a 1<sup>st</sup> and 2<sup>nd</sup> swelling experiment. C) Equilibrium swelling variation ( $\Delta ESR$ ) versus %DAT:**

1 after consecutive swelling/deswelling experiments in HGs containing AEMA (squares); and  
2 between HGs containing AEMA and free of AEMA (circles).  
3

4 Since HGs will be later treated with aqueous solutions of sodium periodate,  
5 understanding how water diffuses into the hydrogels could be useful to interpret how the  
6 post-synthesis modification proceeds. For this reason, the swelling kinetics were studied  
7 to determine the diffusion mechanism of water into the matrix, and the effect of the  
8 percentage of cross-linker used. The swelling kinetic of HGs is closely related to their  
9 morphology, to viscous interaction between polymer and solvent, and to polymer-  
10 polymer interactions.<sup>38</sup> Except for their morphology, the rest of the characteristics  
11 depend on the polymer chemical functionality and cross-linking degree. The swelling  
12 rate (SR) over time in p-AM-AEMA-BIS-DAT HGs is shown in Figure 3A. During their  
13 swelling, the gels incorporate water quickly at short times, but the swelling rate  
14 decreases sharply after reaching 90% of the equilibrium swelling. In general, they reach  
15 50% of the final swelling in approximately 1.5 h, while 95% is achieved in 5 h. This data  
16 was used to determine the type of water diffusion mechanism within HGs using  
17 Equation 3 (see Materials and Methods). For cylindrical HGs, the theory indicates that: if  
18  $0 < n < 0.5$ , the diffusion mechanism of the solvent follows a Fickian behavior, in which  
19 only the diffusion rate of the solvent within the matrix is the determinant process; if  
20  $0.5 < n < 1$ , it represents a non-Fickian diffusion mechanism in which not only the diffusion  
21 of the solvent is relevant, but also the relaxation kinetics of the polymer chains; if  $n = 1$ ,  
22 it corresponds to a type II mechanism, in which the swelling kinetic is determined by the  
23 speed of relaxation of the chains.<sup>37</sup> The results indicate that the dominant type diffusion  
24 of water corresponds to a non-Fickian mechanism in all cases, with values of  $n \approx 0.63$ ,

1 regardless of the degree of cross-linking of the polymers (Figure 3B). These results  
2 confirm that the degree of cross-linking did not affect the relation between water  
3 diffusion and chains mobility, despite the previously observed ESR differences.

4



5

6 **Figure 3. A) Swelling kinetics of p-AM-AEMA-BIS-DAT in water. B) Exponent  $n$  versus**  
7 **DAT concentration. Straight-line indicate the lineal regression of data and dotted lines**  
8 **shows confidence bands (95%).**

9

10 Later, the effects caused by the diffusion of periodate into the HGs were studied. For  
11 this purpose, fully swollen p-AM-AEMA-BIS-DAT HGs were treated with a sodium  
12 periodate solution and changes in swelling rate were followed over time. The changes  
13 observed in the swelling rate over time ( $SR_t$ ) respect to the initial swelling ratio ( $SR_0$ )  
14 evidenced the cleavage of DAT-crosslinks (Figure 4A and B). In all cases, an increase  
15 in the mass and volume of the HGs was observed during the reaction, until reaching a  
16 plateau in approximately 5 h. In addition, cross-linked networks with a larger amount of  
17 DAT increased the SR up to 40% (see supplementary information, S.I 1). In contrast,

1 networks with low percentage of DAT showed minor increase. When the HG contains  
2 1% DAT (p-AM-AEMA-BIS-DAT(1)) the SR index increased only  $\approx 3\%$ . These  
3 observations indicate that increasing amounts of DAT were effectively incorporated in  
4 the HGs during the synthesis. Moreover, the periodate-mediated cleavage of DAT-  
5 crosslinks proceeded selectively, without affecting BIS-crosslinks.

6 We have previously observed that the periodate cleavage seemed to occur fast, from  
7 the outer layers to the core, upon diffusion of the periodate ion into the  
8 network.<sup>39</sup> Similarly, Plunkett and collaborators previously reported that the kinetics of  
9 periodate-mediated oxidation of glycol pendant groups inside of polymeric hydrogels  
10 competed with the diffusion rate of the oxidant into the network, to determine the global  
11 kinetics of the reaction. Moreover, they exploited this feature to promote a superficial  
12 modification of the HGs.<sup>40</sup> In our case, the kinetic dependence of DAT-cleavage upon  
13 periodate diffusion was reflected in the obtained results (see S.I 1). The rate of change  
14 of SR with the reaction time showed a clear dependency with the amount of DAT in the  
15 HGs. Considering that an excess of periodate was used in all the cases, and that all the  
16 networks previously showed a similar diffusion behavior despite their crosslinking  
17 degree, the higher rate of change in  $SR_t/SR_0$  observed for HGs with greater amounts of  
18 DAT seems to be related to a faster reaction rate caused by a larger amount of DAT-  
19 crosslinks in the way of the diffusional front (see S.I 1).

20 Based on those findings, a kinetic model in order to correlate the reaction kinetic of diol  
21 cleavage with the observed swelling rate changes over time (see S.I 2) was proposed.  
22 Considering that an excess of periodate was used to perform the cleavage reactions, a  
23 pseudo-first order kinetic dependence of the reaction rate with respect to the amount of  
24 DAT-crosslinks was observed:



1

2  $v = k' \cdot [R_1 - DAT - R_2]$  ; where  $k' = k \cdot [IO_4^{-1}]$  (Equation 4)

3

4 Furthermore, considering that the concentration of aldehydes yielded during the  
5 reaction is associated with the number of broken DAT-crosslinks, and that both are  
6 simultaneously related to the swelling rate of the networks, the following mathematical  
7 equation was **obtained** (o proposed?) in order to model the swelling rate changes over  
8 time, during the reaction with periodate:

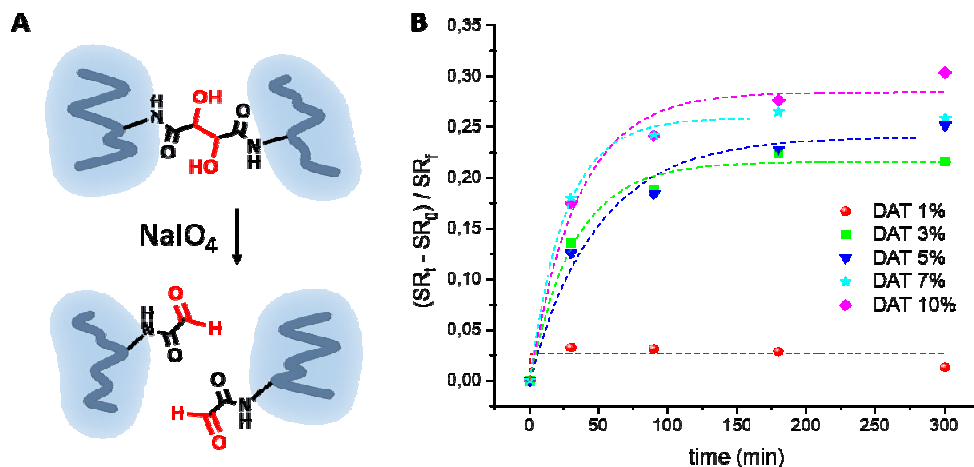
9

10  $SR_t = k'' \cdot (1 - e^{-k' \cdot t}) + SR_0$  (Equation 5)

11

12 The equation was applied to fit the experimental results (figure 4B, dashed line). In  
13 summary, the previous observations support the idea that the diffusion of periodate is  
14 determinant for the overall reaction rate, while the periodate-mediated cleavage of the  
15 diols occurs relatively fast. So, under the studied reaction conditions for these materials,  
16 the cleavage reaction kinetic seems to be according to a pseudo-first order behavior,  
17 with respect to DAT-crosslinks,.

18

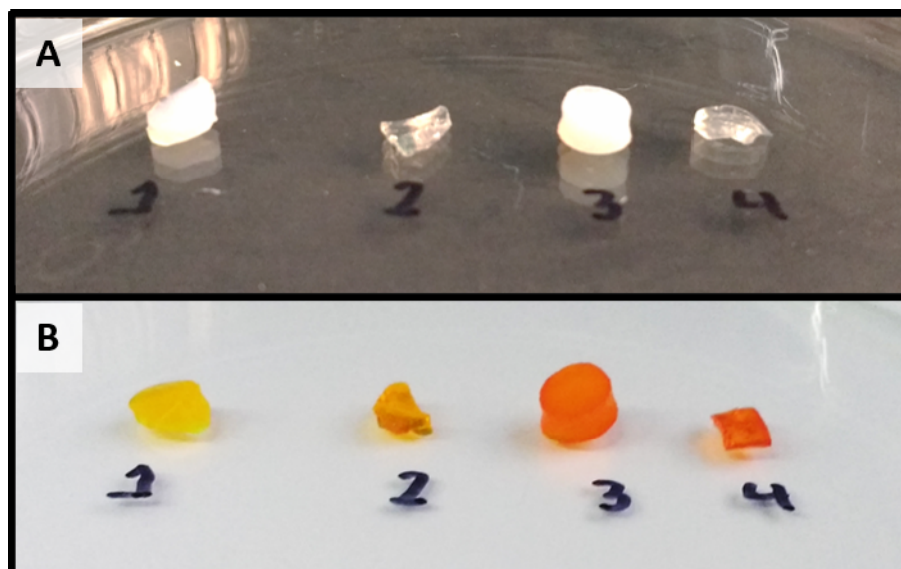


1  
 2 **Figure 4 – A) Scheme showing the cleavage of DAT-crosslinks. B) Relative SR index as a**  
 3 **function of periodate reaction time for p-AM-AEMA-BIS-DAT HGs. Dotted lines indicate**  
 4 **the adjust of data with equation 5.**

5  
 6 We have previously reported that the combination of BIS and DAT cross-linking agents  
 7 enabled the treatment of gels with sodium periodate to generate a selective breakdown  
 8 of DAT-crosslinks, without affecting BIS-crosslinks, as well as obtaining aldehyde  
 9 groups into the network.<sup>24</sup>The only way to recover part of the crosslinking points cleaved  
 10 by periodate was by the external addition of a difunctionalized cross-linker, such as a  
 11 dihydrazide functionalized molecule, capable of forming covalent bonds with the  
 12 pendant aldehyde FGs.<sup>24,41</sup>However, in this case, the presence of amino groups, due to  
 13 AEMA incorporation in the HGs, could enable obtaining self-healing materials based on  
 14 imine covalent bonds without externally adding a new cross-linker in a subsequent step.  
 15 To prove this hypothesis, tests were first performed to determine the presence of  
 16 amines and of  $\alpha$ -oxo-aldehyde groups in the HGs, after their treatment with periodate.  
 17 Initially, to demonstrate the presence of amine FGs, a chemical test for the reactivity of  
 18 amines against picryl sulfonic acid (TNBS) was performed. This reagent, which has a

1 yellow color in solution, reacts with primary amine groups to form orange colored  
2 compounds, allowing a qualitative visual detection (Figure 5). HGs containing amino (p-  
3 AM-AEMA-BIS-DAT(10)) and those without amine groups (p-AM-BIS-DAT(10)), as well  
4 as their respective periodate oxidized products (p-AM-AEMA-BIS- $\alpha$ -oxo-ALD(10) and p-  
5 AM-BIS- $\alpha$ -oxo-ALD(10), respectively) were assayed (Figure 5A). The coloration  
6 observed after the reaction with TNBS indicated the absence of amino in p-AM-BIS-  
7 DAT(10) (negative control) and p-AM-BIS- $\alpha$ -oxo-ALD(10), in which only the typical  
8 yellow color of the TNBS solution was observed (Figure 5B, sample 1 and 2,  
9 respectively). In contrast, an intense orange color was observed in p-AM-AEMA-BIS-  
10 DAT(10) and p-AM-AEMA-BIS- $\alpha$ -oxo-ALD(10) (Figure 5B, samples 3 and 4,  
11 respectively), after their reaction with TNBS.

12



13

14 **Figure 5 - Identification test of amino groups performed over p-AM-BIS-DAT(10) (1), p-AM-BIS- $\alpha$ -**  
15 **oxo-ALD(10) (2), p-AM-AEMA -BIS-DAT(10) (3), and p-AM-AEMA-BIS- $\alpha$ -oxo-ALD(10) (4); A)**  
16 **Samples before TNBS addition; B) Samples after reaction with TNBS.**

17

1 Later, an FT-IR study of p-AM-AEMA-BIS-DAT(10) was performed before and after its  
2 modification with periodate, and compared with the absorption spectrum of the cross-  
3 linking agent DAT. Figure 6 shows the FT-IR spectra of the samples. The signals at  
4 1061 and 1125  $\text{cm}^{-1}$  assigned to the C-O stretching in alcohols, and the wide signal  
5 between 3650 and 3200  $\text{cm}^{-1}$ , characteristic of O-H stretching, are present in both  
6 products, indicating the incorporation of the cross-linker. In addition, the signal assigned  
7 to the deformation outside the plane of the -CH belonging to DAT vinyl groups (918  $\text{cm}^{-1}$ )  
8 was not observed in the HGs, denoting the incorporation of the cross-linker into the  
9 network. We have previously reported that the rupture of DAT in aqueous medium leads  
10 to formation of hydrated aldehyde groups (geminal diol).<sup>24</sup> This, explains the absence of  
11 characteristic bands of aldehyde groups in p-AM-AEMA-BIS- $\alpha$ -oxo-ALD (10) spectrum,  
12 and the presence of characteristic bands of alcohol groups, after periodate-mediated  
13 cleavage of the cross-links. The signals generally observed in amines are overlapped  
14 by the absorption bands of other FGs: the stretching of -NH<sub>2</sub> (3500 to 3200  $\text{cm}^{-1}$ ) is in  
15 the region of intense absorbance of O-H stretching; the deformation signal of -NH<sub>2</sub>  
16 (1610  $\text{cm}^{-1}$ , absent in DAT but present in both HGs) could correspond to both p-AEMA  
17 and p-AM amide. In the same way, the signal corresponding to C=N stretching of imines  
18 is generally observed in the region of 1690 to 1520  $\text{cm}^{-1}$ , which overlaps with the  
19 stretching region of C=O bonds, in which carbonyl groups from AM, AEMA, BIS, DAT or  
20 from its oxidation product may be absorbing.

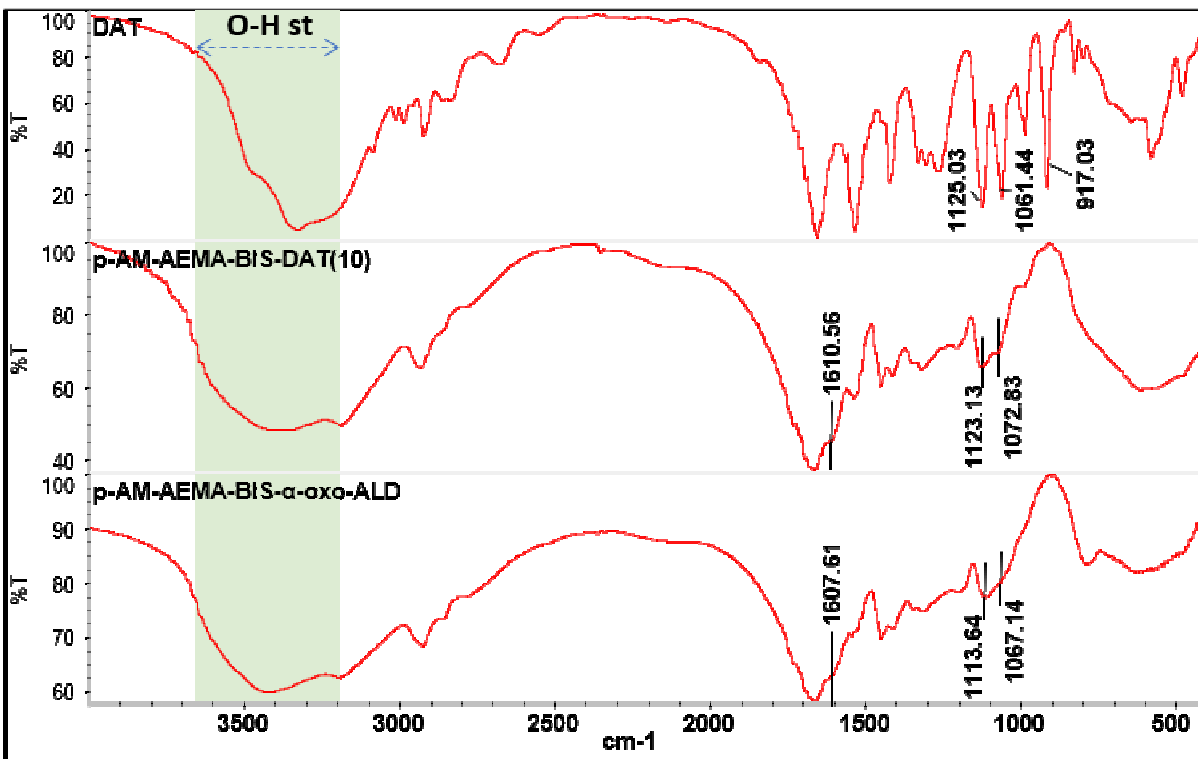


Figure 6 - FT-IR of DAT, p-AM-AEMA-BIS-DAT (10), and p-AM-AEMA-BIS- $\alpha$ -oxo-ALD (10).

1  
 2  
 3  
 4 p-AM-AEMA-BIS- $\alpha$ -oxo-ALD(10) was then studied by NMR to characterize the chemical  
 5 nature of polymer network after oxidation with periodate. To perform this procedure, the  
 6 gel was lyophilized, grinded, and finally rehydrated in D<sub>2</sub>O. The <sup>1</sup>H-NMR spectrum can  
 7 be observed in Figure 7. The wide signals are a typical indication of low mobility chains,  
 8 due to the cross-linked structure of the polymer. However, various signals are clearly  
 9 distinguished as those of backbone at 1.70 ppm (-CH<sub>2</sub>) and 2.29 ppm (-CH-) and those  
 10 belonging to amide (-NH<sub>2</sub>) of p-AM at 7.09 and 7.82 ppm.<sup>42,43</sup> Furthermore, two small  
 11 shoulders indicated the presence of aldehydes in the polymeric network: the peak at  
 12 5.33 ppm corresponding to the H of hydrated aldehyde group (-CH(OH)<sub>2</sub>), and the  
 13 signal at 3.23 ppm, providing from the H of methylene, which is adjacent to amide in the  
 14 aldehyde pendant groups (-CH<sub>2</sub>-NH-R).<sup>24</sup>

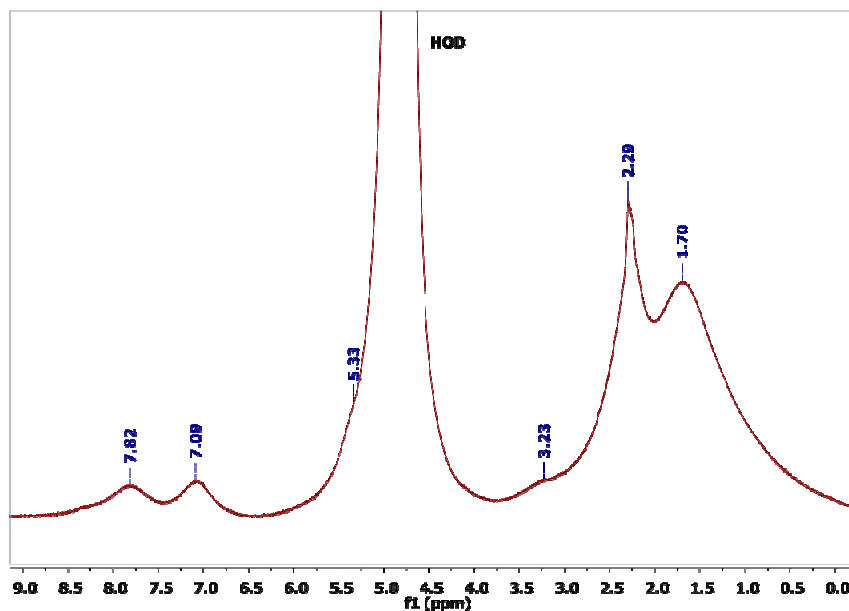
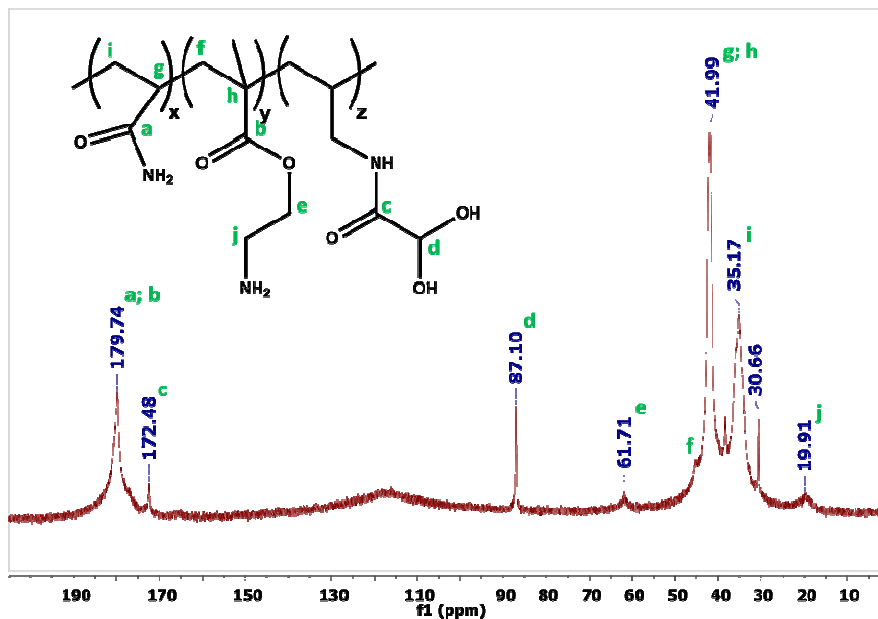


Figure 7 - <sup>1</sup>H-NMR spectrum of p-AM-AEMA-BIS- $\alpha$ -oxo-ALD (10) in D<sub>2</sub>O.

Moreover, the signals in the <sup>13</sup>C spectrum can be more clearly distinguished, due to the C-H decoupling used in the method (Figure 8). The characteristic signals from p-AM backbone (signals *i* and *g* in Figure 8) and amide (signal *a*) are observed.<sup>42</sup> In addition, signals at 87.10 ppm (-CH(OH)<sub>2</sub>) and 172.48 ppm (-NH-C(O)-CH(OH)<sub>2</sub>), indicate the formation of hydrated  $\alpha$ -oxo-aldehyde groups, as it has been previously reported for other equivalent molecules.<sup>44</sup> The signals *j* and *e* in the Figure 8 corroborate the incorporation of the AEMA monomer into the polymer network.<sup>45</sup> The low proportion of AEMA monomer used in the synthesis (5% mol) correlates with the low intensity of its signals with respect to others. In addition, the signal of greater intensity in p-AEMA corresponds to its quaternary carbon (*h*), while the others are usually less intense.<sup>45</sup> Moreover, no signals indicating the possible presence of imines (in the range of 150 to 180 ppm) or stable hemiaminals (60 to 90 ppm) were observed.<sup>46</sup> However, this does not imply their absence, but it should be considered that the imines /

1 hemiaminals formed would be in a low proportion, even less than AEMA, making their  
2 detection difficult with this spectroscopic technique.

3



4

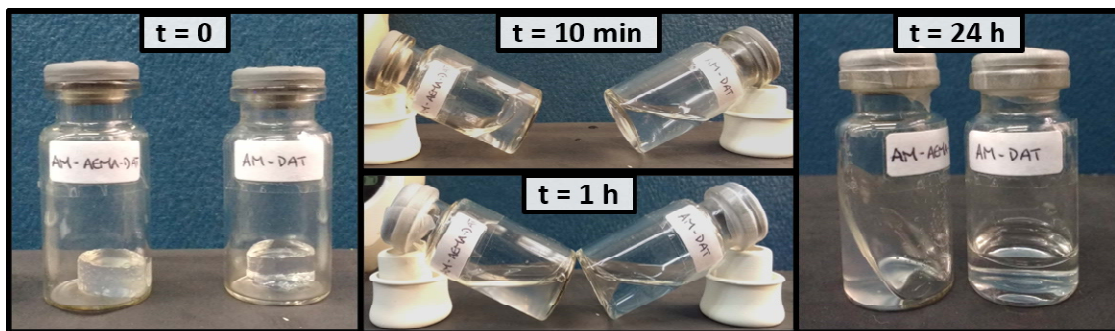
5 **Figure 8 -  $^{13}\text{C}$ -NMR spectrum of p-AM-AEMA-BIS- $\alpha$ -oxo-ALD (10) in  $\text{D}_2\text{O}$ .**

6

7 The AM-BIS-AEMA-DAT HGs demonstrated the formation of amines and  $\alpha$ -oxo-  
8 aldehydes in the network upon periodate treatment, and were convenient to study how  
9 the diffusion of periodate promotes changes in the swelling capacity due to the cleavage  
10 of DAT-crosslinks. However, the presence of BIS-crosslinks promote slow mobility of  
11 the polymer chains and difficult the formation of imine bonds. For this reason, we next  
12 aimed to obtain materials with superior mobility in the polymer chains, to show  
13 pronounced smart changes in response to periodate treatment and by imine formation.  
14 Consequently, HGs cross-linked only by DAT were synthesized and further studied. For  
15 comparison, AEMA-containing HGs (p-AM-AEMA-DAT(10)) and HGs without AEMA (p-  
16 AM-DAT(10)) were treated with a solution of sodium periodate. Photographs taken

1 during the reaction of the HGs against sodium periodate, at different times, are shown in  
2 Figure 9. Before starting the reaction, the HGs discs fully swollen in water can be  
3 observed ( $t = 0$ ). After adding a periodate solution, a gradual digestion of HGs was  
4 noticed during the first hour of reaction. Meanwhile, the HGs were completely digested  
5 to yield viscous liquids. In both cases, the materials remained in a liquid state for at  
6 least 8 h. However, as expected, a viscosity increase was observed in p-AM-AEMA- $\alpha$ -  
7 oxo-ALD(10).

8



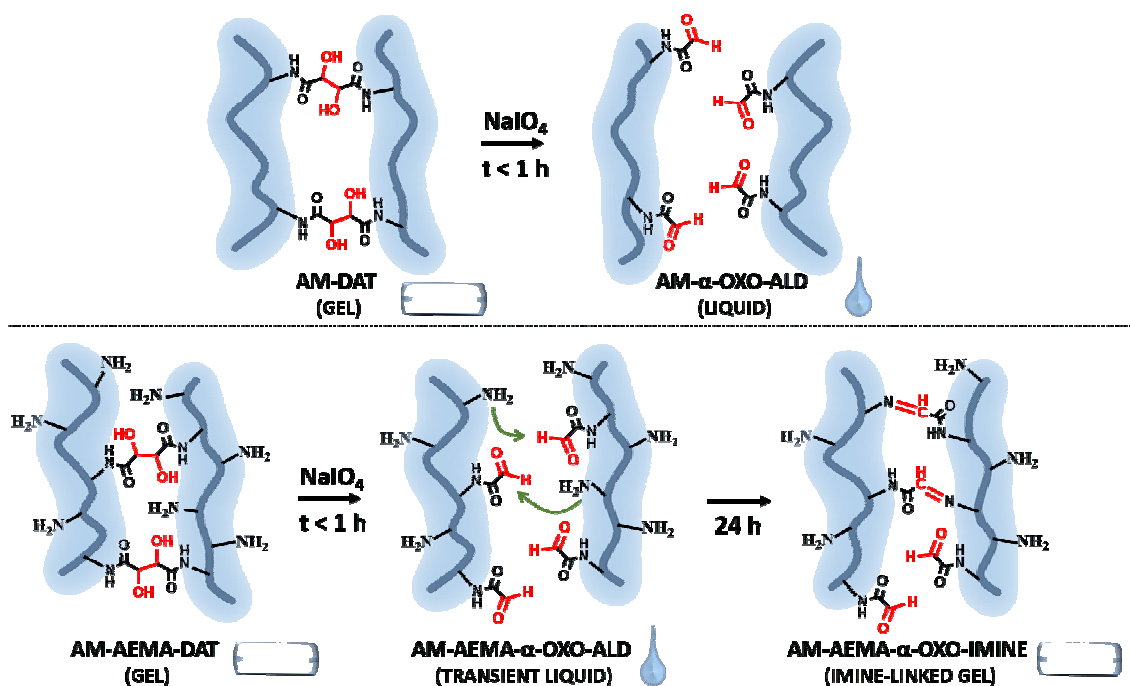
9

10 **Figure 9. Photographic sequence of cleavage and self-healing in p-AM-AEMA-DAT and its**  
11 **comparison with p-AM-DAT. Si puedes pegale arriba de la etiqueta un cartel de texto con el**  
12 **nombre porque no se lee bien (similar a lo que hiciste con el tiempo)**

13

14 Finally, after 24 h, the polymer containing amino groups self-healed yielding a new HG,  
15 while p-AM- $\alpha$ -oxo-ALD (10) maintained a liquid state. This behavior indicated that the  
16 presence of amino and  $\alpha$ -oxo-aldehyde groups generates strong imine interactions that  
17 led to the reparation of the three-dimensional polymer network (Figure 10).





1  
 2 **Figure 10) Schematic representation of cross-linking cleavage in p-AM-AEMA-DAT(10) and p-AM-**  
 3 **DAT(10) and their evolution over time.**

4  
 5 To verify the chemical nature of the interactions in p-AM-AEMA- $\alpha$ -oxo-ALD (10), 0.2 mL  
 6 of the digested polymer (prior to gelation over time) was diluted in  $\text{D}_2\text{O}$  into an NMR  
 7 tube and measured after 24 h.  
 8 The spectroscopic measurement exhibited a more defined spectrum than the previously  
 9 obtained in p-AM-AEMA-BIS- $\alpha$ -oxo-ALD(10), given great chain mobility and  
 10 homogeneity of the sample. In the spectrum (Figure 10) signals due to p-AM are clearly  
 11 distinguished: H of the backbone at 1.65 and 1.76 ppm ( $-\text{CH}_2-$ ); 2.19 and 2.33 ppm ( $-\text{CH}-$ ), and H of the amide at 7.82 and 7.09 ppm ( $-\text{NH}_2$ ). In addition, signals  
 12 corresponding to p-AEMA are observed: 1.19 ppm ( $-\text{CH}_3$  attached to main chain) and  
 13 3.35 ppm ( $-\text{CH}_2-\text{NH}_2$ ).  
 14

1 Furthermore, signals at  $\approx 5.29$  ppm from  $\alpha$ -oxo-aldehyde FGs, are present. Part of  
2 these aldehyde groups are anchored to the network, evidenced by the signal at 3.21  
3 ppm, corresponding to the methylene adjacent to the amide [-CH<sub>2</sub>-NH-C(O)CH(OH<sub>2</sub>)].  
4 The other part corresponds to vinyl aldehyde groups, generated after the treatment with  
5 periodate from DAT units possibly joined only by one vinyl end to the polymer matrix  
6 (signals at 5.86 and 5.21 ppm of vinyl H; signal at 3.85 ppm of the methylene adjacent  
7 to the amide).

8 The reaction of  $\alpha$ -oxo-aldehyde with amino FGs to yield imine bonds was evidenced by  
9 the appearance of a signal at 7.67 ppm (-CH=NH-). This chemical shift is similar to that  
10 reported by Hoefnagel and collaborators in the formation of an imine between glyoxylic  
11 acid (an  $\alpha$ -oxo-aldehyde) and N-methylamine (7.69 ppm).<sup>46</sup>

12 Therefore, the observations made on the cleavage reactions of p-AM-DAT(10) and p-  
13 AM-AEMA-DAT(10) and the subsequent spectroscopic characterization of p-AM-AEMA-  
14  $\alpha$ -oxo-ALD(10) demonstrate the formation of imine bonds in the HGs containing amino  
15 FGs, triggered by the generation of  $\alpha$ -oxo-aldehyde groups by the oxidative cleavage of  
16 DAT with sodium periodate.

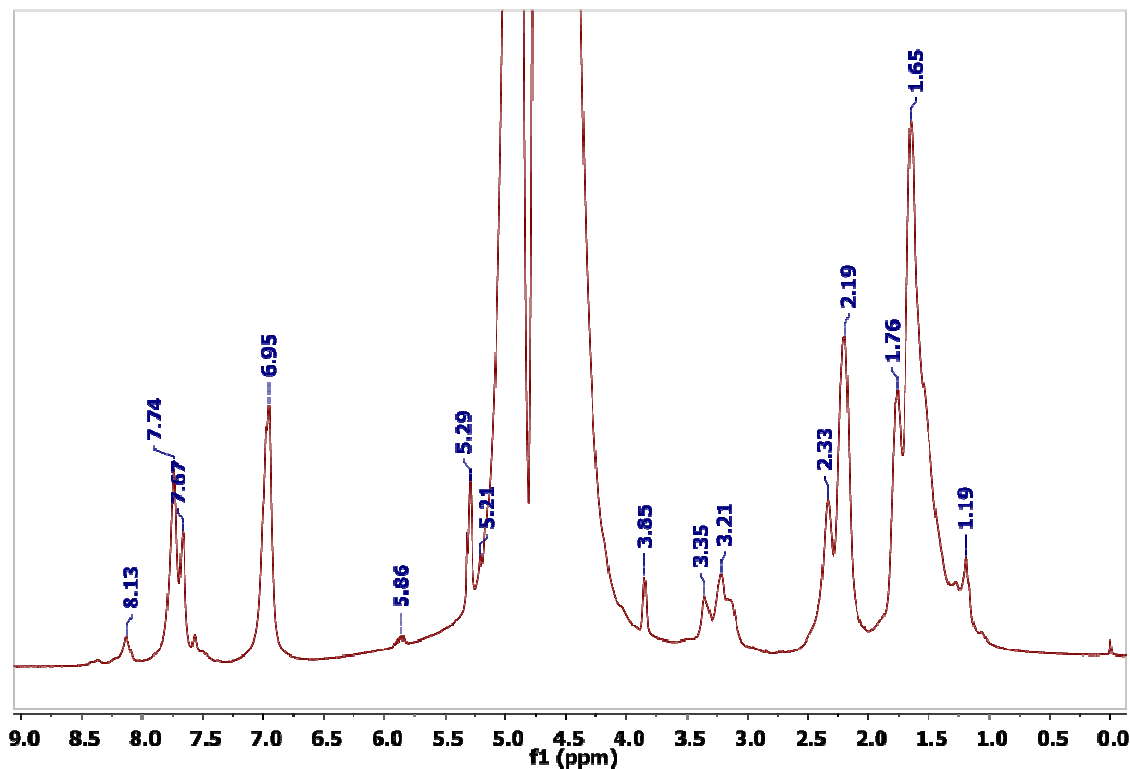


Figure 10 - <sup>1</sup>H-NMR of p-AM-AEMA-BIS- $\alpha$ -oxo-ALD(10).

#### 4. CONCLUSIONS

New hydrogels (HG) based on acrylamide (AM), 2-aminoethyl methacrylate (AEMA) and (+)-*N,N'*-diallyltartardiamide (DAT) as crosslinker, in presence or absence of *N,N'*-methylene bis(acrylamide) (BIS) were developed, envisioning the obtainment of self-healing materials. The studies showed that an increasing incorporation of DAT crosslinker limited the expansion capacity of the network but did not significantly affected water or periodate diffusion. In addition, the use of AEMA seemed to increase the incorporation of DAT, which enlarged the ESR dependency with DAT concentration. The post-synthetic modification of HGs with sodium periodate solutions caused the selective cleavage of DAT-crosslinks producing changes in the swelling properties.

1 Moreover, the magnitude and rate of the SR changes showed dependency with the  
2 number of DAT-crosslinks present in the network.

3 The presence of amino FGs in the HGs, together with  $\alpha$ -oxo-aldehyde FGs obtained by  
4 DAT cleavage, led to the formation of new imine bonds, as it was verified by  $^1\text{H-NMR}$ .

5 Moreover, it was observed that imine bonds were slowly formed in comparison with  
6 oxidative diol cleavage. The combined effect of the kinetics of both reactions enabled  
7 the complete break of the HGs structure in presence of periodate, giving a transient  
8 liquid material, which later responded giving a self-healed HGat room temperature.

9 Future studies will focus on the characterization of the kinetic of the gelation process  
10 promoted by imine bonds, effects of the density of the involved FGs, the recovery of the  
11 mechanical strength, and applications in tissue engineering. In conclusion, the chemical  
12 strategy proposed in this work can be applied to design materials with smart properties  
13 for specific applications.

14

## 15 **5. ACKNOWLEDGMENTS**

16 Authors acknowledge to Consejo Nacional de Investigaciones Científicas y Técnicas  
17 (CONICET), Secretaría de Ciencia y Técnica of Universidad Nacional de Córdoba  
18 (SECyT-UNC) and Fondo para la Investigación Científica y Tecnológica (FONCyT) for  
19 their financial assistance. A. Wolfel thanks CONICET for the endowment of a fellowship.

20

## 21 **6. REFERENCES**

22 1. Kamila, S. Introduction, Classification and Applications of Smart Materials: an Overview.  
23 *Am. J. Appl. Sci.* **10**, 876–880 (2013).

24 2. Mahinroosta, M., Jomeh Farsangi, Z., Allahverdi, A. & Shakoori, Z. Hydrogels as

- 1 intelligent materials: A brief review of synthesis, properties and applications. *Mater.*  
2 *Today Chem.***8**, 42–55 (2018).
- 3 3. Buwalda, S. J. *et al.* Hydrogels in a historical perspective: From simple networks to smart  
4 materials. *J. Control. Release***190**, 254–273 (2014).
- 5 4. Hornat, C. C. & Urban, M. W. Shape memory effects in self-healing polymers. *Prog.*  
6 *Polym. Sci.***102**, 101208 (2020).
- 7 5. Wittmer, A., Wellen, R., Saalwächter, K. & Koschek, K. Moisture-mediated self-healing  
8 kinetics and molecular dynamics in modified polyurethane urea polymers. *Polymer*  
9 *(Guildf)*.**151**, 125–135 (2018).
- 10 6. Krogsgaard, M., Behrens, M. A., Pedersen, J. S. & Birkedal, H. Self-Healing Mussel-  
11 Inspired Multi-pH-Responsive Hydrogels. *Biomacromolecules***14**, 297–301 (2013).
- 12 7. Hu, L., Cheng, X. & Zhang, A. A facile method to prepare UV light-triggered self-healing  
13 polyphosphazenes. *J. Mater. Sci.***50**, 2239–2246 (2015).
- 14 8. Taylor, D. L. & in het Panhuis, M. Self-Healing Hydrogels. *Adv. Mater.***28**, 9060–9093  
15 (2016).
- 16 9. Mathew, A. P., Uthaman, S., Cho, K. H., Cho, C. S. & Park, I. K. Injectable hydrogels for  
17 delivering biotherapeutic molecules. *Int. J. Biol. Macromol.***110**, 17–29 (2018).
- 18 10. Wojtecki, R. J., Meador, M. a & Rowan, S. J. Using the dynamic bond to access  
19 macroscopically responsive structurally dynamic polymers. *Nat. Mater.***10**, 14–27 (2011).
- 20 11. Nevejans, S. *et al.* The challenges of obtaining mechanical strength in self-healing  
21 polymers containing dynamic covalent bonds. *Polymer (Guildf)*.**179**, 121670 (2019).
- 22 12. Krishnakumar, B. *et al.* Vitrimers: Associative dynamic covalent adaptive networks in  
23 thermoset polymers. *Chem. Eng. J.***385**, 123820 (2020).
- 24 13. Tu, Y. *et al.* Advances in injectable self-healing biomedical hydrogels. *Acta Biomater.***90**,  
25 1–20 (2019).
- 26 14. Imines. *IUPAC Compendium of Chemical Terminology***2**, 2957 (2014).

- 1 15. Belowich, M. E. & Stoddart, J. F. Dynamic imine chemistry. *Chem. Soc. Rev.***41**, 2003  
2 (2012).
- 3 16. Kölmel, D. K. & Kool, E. T. Oximes and Hydrazones in Bioconjugation: Mechanism and  
4 Catalysis. *Chem. Rev.***117**, 10358–10376 (2017).
- 5 17. Spears, R. J. & Fascione, M. A. Site-selective incorporation and ligation of protein  
6 aldehydes. *Org. Biomol. Chem.***14**, 7622–7638 (2016).
- 7 18. Lei, X., Huang, Y., Liang, S., Zhao, X. & Liu, L. Preparation of highly transparent, room-  
8 temperature self-healing and recyclable silicon elastomers based on dynamic imine bond  
9 and their ion responsive properties. *Mater. Lett.***268**, 127598 (2020).
- 10 19. Wang, P. *et al.* A self-healing transparent polydimethylsiloxane elastomer based on imine  
11 bonds. *Eur. Polym. J.***123**, 109382 (2020).
- 12 20. Liang, R. *et al.* Molecular design, synthesis and biomedical applications of stimuli-  
13 responsive shape memory hydrogels. *Eur. Polym. J.***114**, 380–396 (2019).
- 14 21. Gupta, B., Tummalapalli, M., Deopura, B. L. & Alam, M. S. Preparation and  
15 characterization of in-situ crosslinked pectin-gelatin hydrogels. *Carbohydr. Polym.***106**,  
16 312–318 (2014).
- 17 22. Han, X., Meng, X., Wu, Z., Wu, Z. & Qi, X. Dynamic imine bond cross-linked self-healing  
18 thermosensitive hydrogels for sustained anticancer therapy via intratumoral injection.  
19 *Mater. Sci. Eng. C***93**, 1064–1072 (2018).
- 20 23. Negrell, C., Voirin, C., Boutevin, B., Ladmiral, V. & Caillol, S. From monomer synthesis to  
21 polymers with pendant aldehyde groups. *Eur. Polym. J.***109**, 544–563 (2018).
- 22 24. Wolfel, A., Romero, M. R. & Alvarez Igarzabal, C. I. Post-synthesis modification of  
23 hydrogels. Total and partial rupture of crosslinks: Formation of aldehyde groups and re-  
24 crosslinking of cleaved hydrogels. *Polymer (Guildf)***116**, (2017).
- 25 25. Tolvanen, M. & Gahmberg, C. G. In vitro attachment of mono- and oligosaccharides to  
26 surface glycoconjugates of intact cells. *J. Biol. Chem.***261**, 9546–9551 (1986).

- 1 26. Norgard, K. E. *et al.* Enhanced interaction of L-selectin with the high endothelial venule  
2 ligand via selectively oxidized sialic acids. *Proc. Natl. Acad. Sci. U. S. A.***90**, 1068–1072  
3 (1993).
- 4 27. Zeng, Y., Ramya, T. N. C., Dirksen, A., Dawson, P. E. & Paulson, J. C. High-efficiency  
5 labeling of sialylated glycoproteins on living cells. *Nat. Methods***6**, 207–209 (2009).
- 6 28. Kornýšova, O., Jarmalavičiene, R. & Maruška, A. A simplified synthesis of polymeric  
7 nonparticulate stationary phases with macrocyclic antibiotic as chiral selector for capillary  
8 electrochromatography. *Electrophoresis***25**, 2825–2829 (2004).
- 9 29. Tetala, K. K. R., Chen, B., Visser, G. M. & van Beek, T. a. Single step synthesis of  
10 carbohydrate monolithic capillary columns for affinity chromatography of lectins. *J. Sep.*  
11 *Sci.***30**, 2828–35 (2007).
- 12 30. Khaparde, A., Vijayalakshmi, M. A. & Tetala, K. K. R. Preparation and characterization of  
13 a Cu (II)-IDA poly HEMA monolith syringe for proteomic applications. *Electrophoresis***38**,  
14 2981–2984 (2017).
- 15 31. Balakrishnan, B. & Jayakrishnan, A. Self-cross-linking biopolymers as injectable in situ  
16 forming biodegradable scaffolds. *Biomaterials***26**, 3941–3951 (2005).
- 17 32. Weihang, J., Panus, D., Palumbo, R. N., Tang, R. & Wang, C. Poly(2-aminoethyl  
18 methacrylate) with well-defined chain-length for DNA vaccine delivery to dendritic cells.  
19 *Biomacromolecules***12**, 612–626 (2012).
- 20 33. Bisht, G., Zaidi, M. G. H. & Kc, B. In vivo Acute Cytotoxicity Study of Poly(2-amino ethyl  
21 methacrylate-co-methylene bis-acrylamide) Magnetic Composite Synthesized in  
22 Supercritical CO<sub>2</sub>. *Macromol. Res.***26**, 581–591 (2018).
- 23 34. Chanthaset, N., Ajiro, H., Akashi, M. & Choochottiros, C. A novel comb-shaped  
24 polymethacrylate-based copolymers with immobilized 2,4-dihydroxybenzaldehyde for  
25 antifungal activity. *Polym. Bull.***75**, 1349–1363 (2018).
- 26 35. Farjadian, F., Schwark, S. & Ulbricht, M. Novel functionalization of porous polypropylene

- 1 microfiltration membranes: Via grafted poly(aminoethyl methacrylate) anchored Schiff  
2 bases toward membrane adsorbers for metal ions. *Polym. Chem.***6**, 1584–1593 (2015).
- 3 36. Tigges, T., Hoenders, D. & Walther, A. Preparation of Highly Monodisperse Monopatch  
4 Particles with Orthogonal Click-Type Functionalization and Biorecognition. *Small***11**,  
5 4540–4548 (2015).
- 6 37. Caykara, T., Kiper, S. & Demirel, G. Thermosensitive poly(N-isopropylacrylamide-co-  
7 acrylamide) hydrogels: Synthesis, swelling and interaction with ionic surfactants. *Eur.*  
8 *Polym. J.***42**, 348–355 (2006).
- 9 38. Peters, A. & Candau, S. J. Kinetics of Swelling of Spherical and Cylindrical Gels.  
10 *Macromolecules***21**, 2278–2282 (1988).
- 11 39. Wolfel, A., Romero, M. R. & Alvarez Igarzabal, C. I. Post-synthesis modification of  
12 hydrogels. Total and partial rupture of crosslinks: Formation of aldehyde groups and re-  
13 crosslinking of cleaved hydrogels. *Polymer (Guildf)*.**116**, 251–260 (2017).
- 14 40. Plunkett, K. N., Chatterjee, A. N., Aluru, N. R. & Moore, J. S. Surface-modified hydrogels  
15 for chemoselective bioconjugation. *Macromolecules***36**, 8846–8852 (2003).
- 16 41. Wolfel, A., Romero, M. R. & Alvarez Igarzabal, C. I. Post-synthesis modification of  
17 thermo-responsive hydrogels: Hydrazone crosslinking of  $\alpha$ -oxoaldehyde obtained from  
18 NIPAm-based polymers. *Eur. Polym. J.***112**, 389–399 (2019).
- 19 42. Ziaee, F., Bouhendi, H. & Ziaie, F. NMR study of polyacrylamide tacticity synthesized by  
20 precipitated polymerization method. *Iran. Polym. J. (English Ed)*.**18**, 947–956 (2009).
- 21 43. Bovey, F. A. & Tiers, G. V. D. Polymer NMR spectroscopy. IX. Polyacrylamide and  
22 polymethacrylamide in aqueous solution. *J. Polym. Sci. Part A Gen. Pap.***1**, 849–861  
23 (1963).
- 24 44. El-Mahdi, O. & Melnyk, O.  $\alpha$ -Oxo Aldehyde or Glyoxylyl Group Chemistry in Peptide  
25 Bioconjugation. *Bioconjug. Chem.***24**, 735–765 (2013).
- 26 45. Figueiredo, A. R. P. *et al.* Antimicrobial bacterial cellulose nanocomposites prepared by in



- 1 situ polymerization of 2-aminoethyl methacrylate. *Carbohydr. Polym.***123**, 443–453  
2 (2015).
- 3 46. Hoefnagel, A. J., Peters, J. A. & Vanbakkum, H. The Reaction of Glyoxylic Acid with  
4 Ammonia Revisited. *J. Org. Chem.***57**, 3916–3921 (1992).
- 5